ACS OMEGA

http://pubs.acs.org/journal/acsodf

Article

Simulation Study on the Interaction between Chemically Reacting Double Coal Char Particles

Weiguang Su,[#] Meiyu Shi,[#] Ben Zhang, Wenxin Wang, Xudong Song,[*] and Guangsuo Yu

Cite This: *ACS Omega* 2023, 8, 7913−7921

Read Online

ACCESS | Metrics & More | Article Recommendations

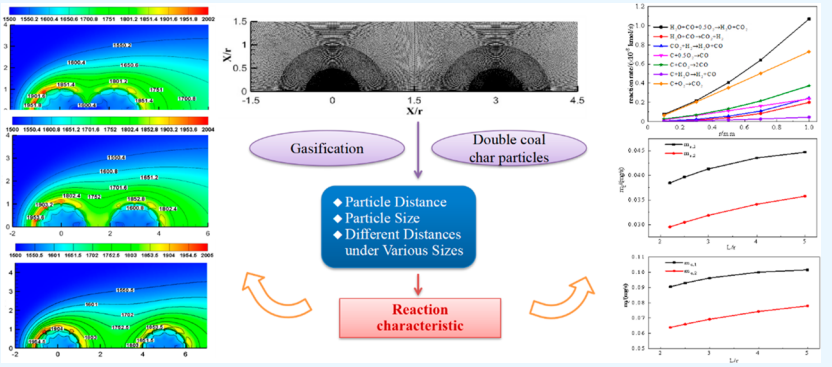

ABSTRACT: Due to the complex atmosphere of the entrained flow gasifier, it is difficult to obtain reactivity properties of coal char particles under high-temperature conditions by experiment. The computational fluid dynamics simulation method is a key way to simulate the reactivity of coal char particles. In this article, the gasification characteristics of double coal char particles under H_2O/O_2/CO_2 atmosphere are studied. The results show that the particle distance (L) has an influence on the reaction with particles. With the gradual increase of L, the temperature first rises and then falls among the double particles due to the migration of the reaction area, and the characteristics of double coal char particles gradually approach that of single coal char particles. The particle size also has an influence on the gasification characteristics of coal char particles. As the particle size varies from 0.1 to 1 mm, the reaction area of particles becomes smaller at high temperature and finally attaches to the surface of the particles. The reaction rate and carbon consumption rate increase with increasing particle size. As the size of double particles is changed, the reaction rate trend of double coal char particles at the same particle distance is basically the same, but the change degree of reaction rate is different. With the increase of the distance between coal char particles, the change of the carbon consumption rate is larger for the small particle size.

1. INTRODUCTION

China's main source of energy production is coal.[1,2] It is the world's largest coal producer and consumer.[3] In the past, coal was used only for heating, which would cause serious environmental pollution. With the progress of science and technology, coal is now used to synthesize new substances through different technologies to achieve more efficient utilization, which not only slows down the pollution caused by coal combustion but also produces more new energy for other industries.

Coal gasification technology can convert low-quality coal, petroleum char, and other materials into syngas, as one of the important technologies of clean coal utilization technology.[4,5] The coal gasification technology can not only be used in the production of coal-based chemicals, coal-based fuel oil, fuel cells, and hydrogen but also be applied to integrated gasification combined cycle (IGCC) power generation, which is the common and leading technology in these industries.[6−8] Entrained-flow gasification is characterized by high carbon conversion rate, strong production capacity, and wide adaptability of coal types. It is a flexible and reliable industrial technology and has become mainstream in the gasification process.[9] The gasifier occupies an important position in the process of coal gasification technology. At present, the stable operation of the gasifier has been widely considered. As one of the main components of the gasification reaction, the high-temperature particles in the entrained-flow gasification have various characteristics closely related to the state of the gasifier. The temperature distribution, particle morphology, reaction rate, and other characteristics of the particles in the process of

Received: December 1, 2022
Accepted: February 2, 2023
Published: February 14, 2023

https://doi.org/10.1021/acsomega.2c07675
ACS Omega 2023, 8, 7913−7921

movement in the furnace are closely related to the operating state of the gasifier.

A number of experiments and simulations about coal gasification were executed to study the reaction properties of coal char particles. Senneca et al.[10] established a numerical model to calculate the temperature, oxygen distribution, and internal porosity change caused by devolatilization and carbon combustion under various pyrolysis and combustion conditions. Niksa et al.[11] used optical methods to measure the particle size and velocity of single pulverized coal particles in the combustion process. Subsequently, a great deal of research has also been done on the combustion of single particles. Zhu et al.[12] investigated the ignition and combustion process of three kinds of coal particles with high volatiles under ordinary gravity and microgravity and developed relevant mathematical models to simulate the ignition process of the particles. Si et al.[13] used high-speed imaging technology to calculate the temperature and concentration of soot by recording spectral radiation images of single coal particle combustion.

Many researchers dealt with coal char particles of different sizes in a series of experimental research.[14−17] Different ignition temperature of char, ignition delay time, burning temperature, and burning time were investigated at different environment temperatures. Higuera[18] calculated the combustion rate, resistance, and other parameters of a single coal char particle in O_2 and CO_2. The analysis showed that the particle size had little influence on the particle temperature. Some researchers studied the kinetics of the heterogeneous reaction of single coal particles in a specific environment under the influence of oxidation rate and investigated the combustion characteristics of a particle mass in a high-temperature O_2/CO_2 atmosphere.[19−22] Bejarano et al.[23] studied the influence of different oxygen concentrations on the combustion for single particle coal char characteristics. The combustion temperature, duration, and reactivity of single particle coal char were analyzed.

The particle size is one of the important parameters of the coal char particles. The particle size can affect the reaction rate, the position of the flame layer, the combustion temperature, and other properties. It is important to discuss the influence of particle size change on the model of double coal char particles. Richter et al.[24] analyzed three coal particle trajectories with different sizes and discussed the temperature distribution and concentration distribution. Coetzee et al.[25] investigated the effect of char size on the gasification process for three lignite particles with particle sizes of 75, 20, and 2 mm. The results showed that particle size affected the growth rate of CO_2 gasification over the entire range of pores. With the increase of char particle size, the specific surface area of initial char and the small pore fraction increased. Xue et al.[26] investigated the conversion characteristics of particle size and porosity for a single char particle under the higher-temperature O_2/CO_2 atmosphere.

Most of the studies in the above literature focus on the statistical characteristics of single particle coal char in the gasifier at the microscopic scale; the behavior characteristics of multiparticles at the particle scale is rarely studied. In order to deeply understand the characteristics and mechanism of coal char particles in the gasification reaction process and investigate the interaction between double coal char particles, this work established a simulation study of double particle coal char on the basis of single-particle simulation and investigated the gasification reaction features with different distance for porous spherical particles. To systematically explore the gasification reaction process between double coal char particles, the effects of particle size on temperature distribution, reaction rate, carbon consumption rate, and product concentration distribution of coal char particles at different particle distances are compared.

2. NUMERICAL SIMULATION CONDITIONS

2.1. Particle Numerical Model. The gasification reaction process for coal char particles is simplified into a two-dimensional model by computational fluid dynamics (CFD) tools; the spherical char particles are in a high-temperature stable oxidation environment. The particles are at a rest state, and the gas flows around particles. The gas-phase flow is solved by the Navier−Stokes equation, energy conservation equation, and component conservation equation.[27] The flow of gas is considered as an incompressible fluid. The gas only reacts on the surface and pore surface of the carbon particles, but there is no reaction inside the carbon particles. For the purpose of eliminating the wall influence of the reaction between gas-phase flow and char particles, the calculated area is larger than the particle in comparison with the size of char particles. The structure and composition of coal char particles are more complex, so a simplified particle model is used to represent coal char particles. In this study, coal char particles with low porosity are simulated, and the study assumes that the porous structure of double coal char particles exists only on the outside of the particles, and that the pores are long and uniformly distributed. The porosity is 0.3, the pore radius is 50 μm, and the particle radius is 1/20.

Figure 1 shows the model of double coal char particles with particle distance (L) = 3r and the external region diagram. At

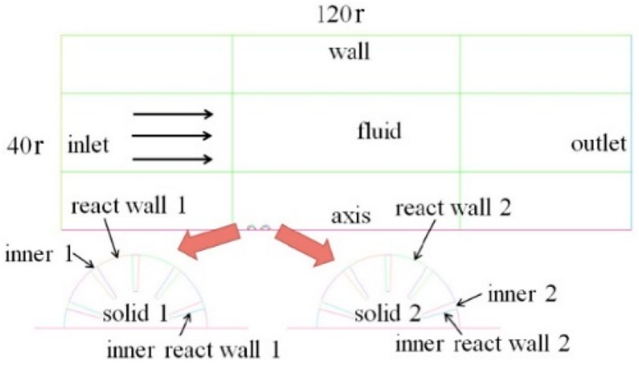

Figure 1. Schematic for model of double coal char particles and external region.

this distance, it is expected that the interaction between the double particles can be well understood. Particle distance (L) is defined as the distance between the double particles' centers. 2r represents the size of the coal char particle. The particle model has symmetry, so only half of the region is selected for simulation calculations. The computational domain is a rectangle with 120r × 4r, and the gas-phase fluid inlet is set on the left side of the domain. In this particle model, the radius of the spherical particle r is set as 1 mm, and the position of the left particle is at the x axis with the center at x = 0. The high-temperature H_2O/O_2/CO_2 atmosphere flows from the inlet to the calculation area at a constant velocity. The structure and size of the double particles in the model are exactly the same,

https://doi.org/10.1021/acsomega.2c07675
ACS Omega 2023, 8, 7913−7921

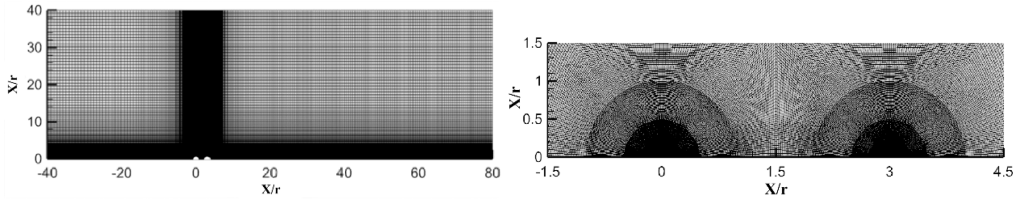

(a) Grid of computational domain (b) Grid of the area around particles

Figure 2. Grid diagram of double coal char particles model.

and the change degree of the double coal char particles size is consistent.

Figure 2 is the grid schematic diagram of the double coal char particle model with particle distance $L = 3r$ and the enlarged grid diagram of the area near the particles. The left particle is defined as particle 1, and the right particle is particle 2. Because the research focuses on coal char particles and its vicinity, the grids of particles and adjacent areas are getting denser. The grid quality of the area near the particle can reach more than 0.9. When the particle model is solved under different boundary conditions, at least 10^5 iterations are carried out to ensure the convergence and accuracy of the calculated results. In the calculation of mass flow in the chemical reaction zone, the Stefan flow and various diffusion equations are also considered.

The expression of the component transport equation is as follows:

$$\nabla(\rho u\omega_i) = -\nabla J_i + R_i + S_i \tag{1}$$

The expression of the law of conservation of mass is

$$\nabla(\rho u_i) = S_m \tag{2}$$

The expression of the Navier−Stokes equation is

$$\rho\frac{\mathrm{d}V}{\mathrm{d}t} = \rho\tau - \nabla p + \mu\nabla^2 V \tag{3}$$

The equation for the stress tensor τ is

$$\tau_{ij} = [\mu(\delta u_i/\delta x_j + \delta u_j/\delta x_i)] - 2\mu(\delta u_i/\delta x_i)\delta_{ij}/3 \tag{4}$$

The energy conservation equation is as follows:

$$\nabla[u(\rho E + p)] = \nabla\left(k_{\mathrm{eff}}\nabla T - \sum_i h_i J_i + u\tau_{\mathrm{eff}}\right) + S_{\mathrm{h}} \tag{5}$$

An expression for energy is given by

$$E = h - p/\rho + u^2/2 \tag{6}$$

The equation for the density of the gas-phase mixture is

$$\rho = p/RT\sum(\omega_i/M_i) \tag{7}$$

where ρ and u are the density and flow velocity of the fluid in the ambient atmosphere. ω_r is the mass fraction of component r in the gas phase. J_i, R_i, and S_i are diffusion flux, reaction generation rate, and input source term of component i. S_{m} is the mass source term, and u is the viscosity coefficient. p is the environmental pressure. V is the velocity vector. μ is the dynamic viscosity, and τ is the stress tensor. k_{eff} is the effective heat conductivity coefficient. h_i is the enthalpy of component i. S_h is the heat of chemical reaction and other customized heat source terms. R is the ideal gas constant, and M_{i} is the relative molecular mass of component i.

2.2. Heterogeneous and Homogeneous Reactions.

The chemical reactions used in the simulation of coal char particles are as follows:[28]

Homogeneous reaction:

$$H_2O + CO + \frac{1}{2}O_2 \rightarrow H_2O + CO_2 \tag{R1}$$

$$H_2O + CO \rightarrow CO_2 + H_2 \tag{R2}$$

$$CO_2 + H_2 \rightarrow H_2O + CO \tag{R3}$$

Heterogeneous reaction:

$$C + \frac{1}{2}O_2 \rightarrow CO \tag{R4}$$

$$C + CO_2 \rightarrow 2CO \tag{R5}$$

$$C + H_2O \rightarrow H_2 + CO \tag{R6}$$

$$C + O_2 \rightarrow CO_2 \tag{R7}$$

In this paper, laminar flow is adopted for the gas-phase fluid. Laminar flow is simpler than turbulent flow, and the calculation of chemical source terms by the Arrhenius equation is more accurate. As shown in Table 1, the Arrhenius equation is used to calculate the chemical reaction rate constant:

$$k_r = \mathrm{A}_r T^n \exp(-E_r/\mathrm{RT}) \tag{8}$$

where A_r is the preindex factor of reaction, E_r is the reaction activation energy (J/mol), and n is the temperature index.

Table 1. Rate Coefficient Parameters of Homogeneous and Heterogeneous Reactions

reaction	ref	A_r	E_r (J/mol)	n
R1	Turns[29]	2.24×10^{12} $m^{2.25}/(kmol^{0.75}\cdot s)$	1.6736×10^8	0
R2	Jones[30]	2.75×10^9 $m^3/(kmol\cdot s)$	8.368×10^7	0
R3	Richter[21]	9.98×10^{10} $m^3/(kmol\cdot s)$	1.205×10^8	0
R4	Caram[31]	3.007×10^5m/s	1.4937×10^8	0
R5	Libby[32]	4.605 m/(s·K)	1.751×10^8	1
R6	Libby[32]	11.25 m/(s·K)	1.751×10^8	1
R7	Date[33]	593.83 m/(s·K)	1.4965×10^8	1

The inlet is velocity inlet, the flow model is laminar, the inlet velocity is 0.5 m/s, and operating pressure is 101325 Pa. The P-1 model is used to simulate the radiation heat transfer. The radiation coefficient of the coal char particles is 0.95, and the wall radiation coefficient is 0.9.

The standard molar enthalpy of reaction for the reaction equation is equivalent to the difference between the standard molar enthalpy of formation of the product and the reactant, which is calculated as

https://doi.org/10.1021/acsomega.2c07675
ACS Omega 2023, 8, 7913−7921

$$\Delta_r H_m^{\Theta} = \sum_B \nu_B \Delta_c H_m^{\Theta}(B) - \sum_A \nu_A \Delta_c H_m^{\Theta}(A) \quad (9)$$

The reaction heat source term S_h in the energy conservation equation is calculated as follows:

$$S_{h,reaction} = \sum_i \left(h_i^{\Theta}/M_i + \int_{T_{ref,i}}^{T} c_{p,i} dT \right) R_i \quad (10)$$

The specific heat capacity $c_{p,i}$ of a single substance i changes with temperature, and the formula is as follows:

$$c_p = \sum_i Y_i c_{p,i}, \qquad c_{p,i} = a_i + b_i T + c_i T^2 d_i T^3 e_i T^4 \quad (11)$$

The P-1 radiation model is used to calculate the radiation source term between the particle and the gas phase and each wall surface of the particle, and the expression is

$$-\nabla q_i = \alpha G - 4\alpha\sigma T^4 \quad (12)$$

The average temperature of the particle's outer surface T_s and carbon consumption per unit time m_c are used to represent the particle reaction characteristics. The calculation formulas are as follows:

$$T_s = \sum_{n=1}^{N} \oint_{s_n} T_{s,n} dS_n / \sum_{n=1}^{N} \oint_{s_n} dS_n \quad (13)$$

$$m_c = \sum_{n=1}^{N} \oint_{S_n} m_{c,n} dS_n \quad (14)$$

where A is the reactant, B the product, and ν the stoichiometric number. h_i^{Θ} is the enthalpy of formation of component i. The specific heat capacity c_p of the mixture can be calculated according to the mixing law and weighted by the group fraction of each substance in the mixture. q_i is radiant heat flux. α is the absorption coefficient. G is incident radiation. σ is Stefan−Boltzmann's constant. $T_{s,n}$ is the average temperature, and $m_{c,n}$ is the carbon consumption rate of the microelement surface.

2.3. Model Validation. Figure 3 presents a comparison of the simulation results with the results of the literature,[34] and

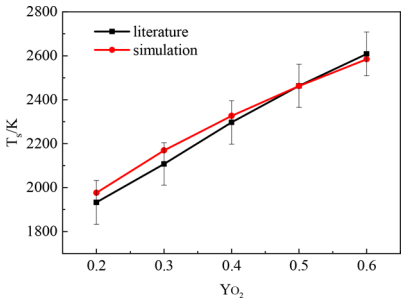

Figure 3. Comparison of simulation results and literature results

the variation curves of coal char particle surface temperature with oxygen concentration are compared. It can be seen that the simulation is consistent with the experimental results, and the values are basically the same. The simulation results are within the error value in the experiment. The validation results show that the porous particle model can better reflect the gasification reaction properties of actual coal char particles.

3. RESULTS AND DISCUSSION

3.1. Particle Distance. This section investigate the gasification reaction characteristics of double coal char under different particle distances. The particle size r of both char particles is 1 mm, and r is the radius of the char particles. (When the radius is small, the oxygen is almost zero inside pores, which inhibits reactions inside the pore.) The environmental temperature T_∞ is 1500 K, the molar fraction ratio of gas is YH_2O: YO_2: YCO_2= 0.1:0.4:0.5, and the particle distances L are 2.2r, 2.5r, 3r, 4r, and 5r.

Figure 4 represents the temperature distribution of double coal char particles with different particle distances. In Figure 4a, it is clear that when L = 2.2r, the high-temperature areas appear near the left-hand (pore) of particle 1 and the right-hand (tail) of particle 2. While in the middle of particles 1 and 2, there appears a relative low-temperature area. The high temperature generated by the reaction of carbon and air flow near the particle surface diffuses into the particle interior. Particle 1 is the main area of gasification reaction due to the full contact between fluid and particles. However, the temperature field at the junction of the double particles is fused and the temperature is relatively low. This is because the particle space is too close, the fluid cannot be diffused out from the particles in time, and the reaction degree is weak. However, when the particle space increases, the temperature field between the double particles change. The temperature in the middle of particles 1 and 2 (low-temperature region in Figure 4a) gradually improves, and the high-temperature region of the double particle coal char expands from the pore to the tail of particle 1. The gas-phase fluid can better contact with the tail of particle 1 due to the increase of particle space, and the reaction region gradually expands to the middle position of particle 1 and particle 2. When the particle space increases to 4r, the temperature fields of the double particles begin to separate. When the particle space is further increased, the reaction characteristics of double coal char particles gradually converge to single particle, but particle 1 still has some influence on the temperature field of particle 2. The overall temperature of particle 1 is always higher than that of particle 2. The blocking of particle 1 inhibits the diffusion of gas-phase fluid near particle 2 and also inhibits the reaction. The high-temperature region of a single particle is concentrated at the pores of the particle, and the external temperature of the particle gradually decreases from inside to outside. The temperature gradient inside the particle is also generated under the influence of the heat produced by the chemical reactions on the face and the pores of the particle. The temperature decreases as it reaches the core of the particle. The peak temperature of the double particle coal char at different particle spacing is basically the same, about 1950 K.

Figure 5 presents the Stefan flow and streamlines distribution of the double coal char particles near the particles at different particle distances. It shows the mass transfer process of the particle face reaction. The streamline in Figure 5 represents the trajectory line of fluid flow, and the intensity indicates the CO and CO_2 molar fraction near the particle, respectively. CO and CO_2 concentrations on the particle surface and pores are both higher than the environmental concentration, suggesting that the oxidation reaction between C and O_2 mainly takes place in the pores and on the face of double coal char particles. The airflow is transferred from high concentration to low concentration. Figure 5a,b shows that

https://doi.org/10.1021/acsomega.2c07675
ACS Omega 2023, 8, 7913−7921

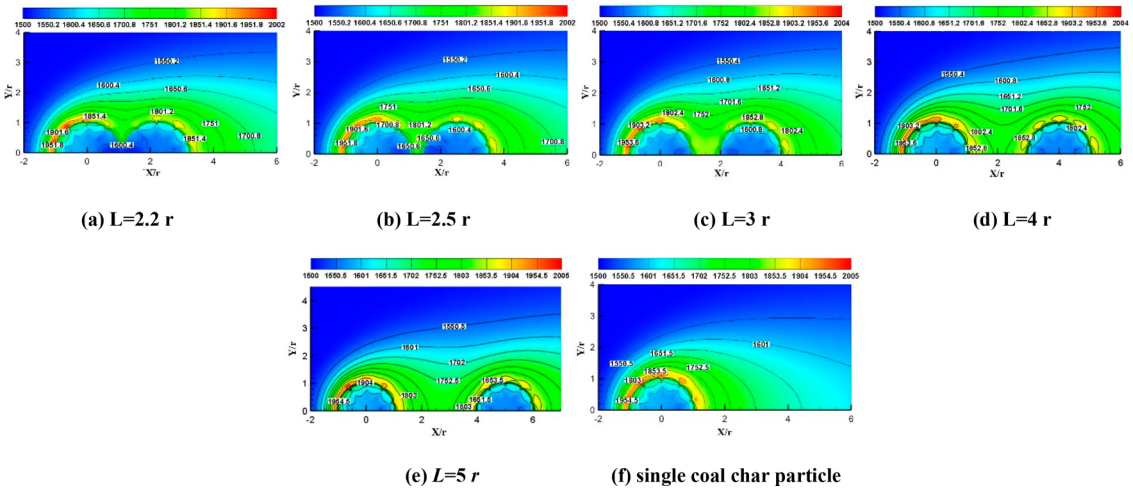

Figure 4. Temperature distribution of double coal char particles under different particle distances

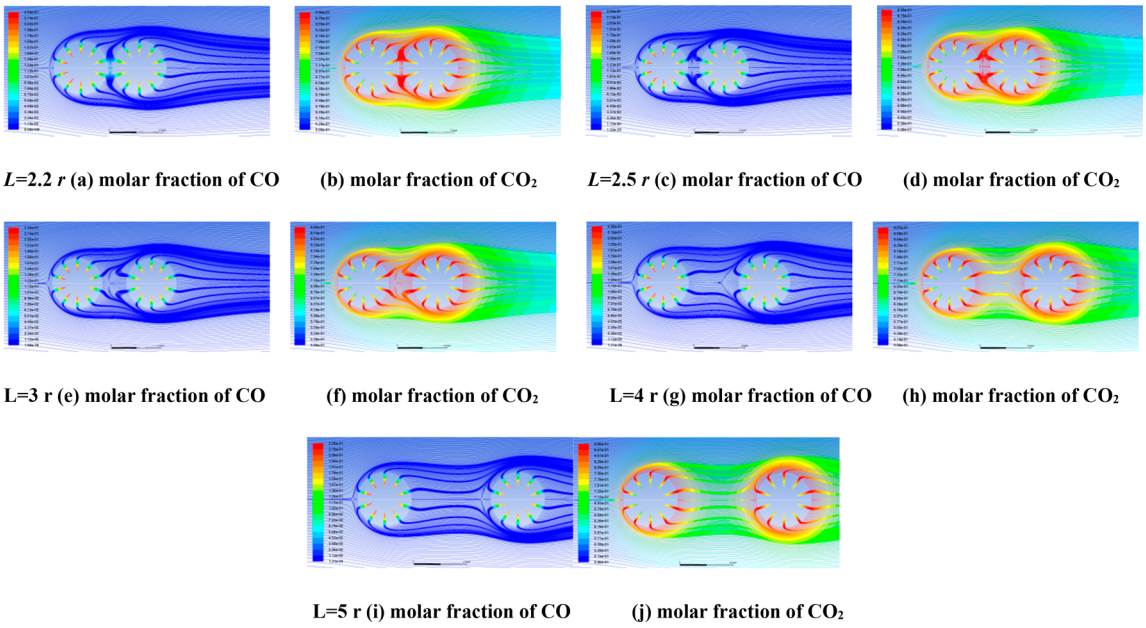

Figure 5. Stefan flow and streamlines around the double coal char particles.

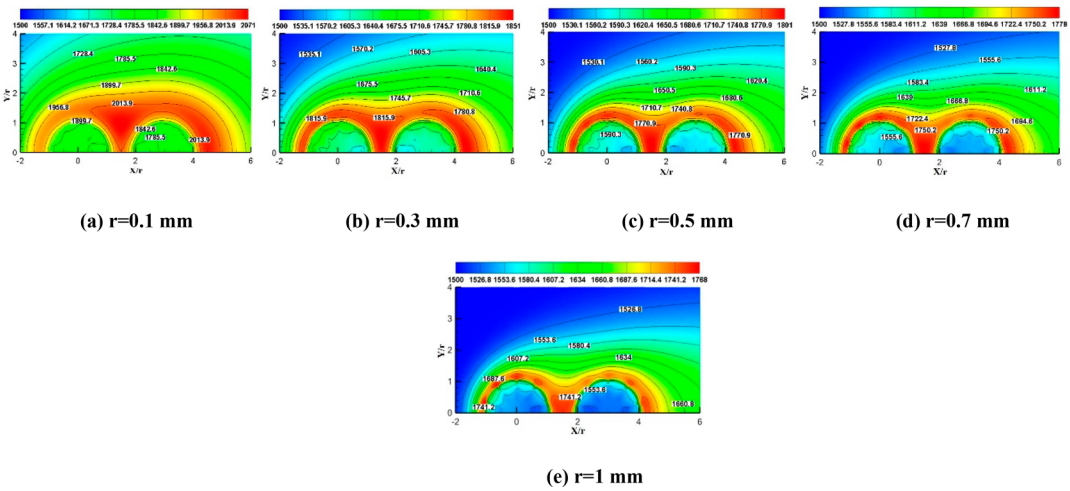

Figure 6. Temperature contour map of double char particles with different particle sizes.

https://doi.org/10.1021/acsomega.2c07675
ACS Omega 2023, 8, 7913−7921

when L = 2.2r, the CO molar fraction at the middle of the double particles is slightly higher than the environmental CO concentration, while the CO_2 molar fraction in the middle is much higher than the environmental CO_2 concentration. When L < 3r, the CO and CO_2 molar fraction of particle 2 is distinctly influenced by the flow field of particle 1. With the increase of particle distance, the molar fraction of both CO and CO_2 in the middle of the double particles decreases. When L = 5r, the effect of particle distance on the two-particle flow field distribution is very low. The highest peak concentration of CO is inside the pores of the particles, and the highest peak concentration of CO_2 is at the surface of the particles. Because the oxygen concentration inside the pores of the particles is low, C is incompletely oxidized to produce CO, releasing low heat. CO diffuses to the particle surface and contacts with sufficient oxygen in the environment to produce CO_2, generating a lot of heat.

3.2. Particle Size. In this section, the difference in the reactive process of double coal char particles is studied in detail when particle size is r = 0.1, 0.3, 0.5, 0.7, and 1 mm. The structure and size of double coal char particles are the same, so the change degree of the particle size of the double particles is also the same. The conditions are that the ambient temperature T_∞ = 1500 K, the proportion of the inlet atmosphere concentration is YH_2O:YO_2:YCO_2 = 0.05:0.2:0.75, and the particle distance L = 3r.

By comparing the temperature field distribution, reaction rate, and carbon consumption rate of double char particles with different particle sizes, the effects of particle size variation on the gasification reaction characteristics for double coal char particles and the reasons for the variations are explored.

Figure 6 represents the temperature distribution contour map of double char particles with different sizes, and the contour maps a−e represent particle temperature with particle sizes from 0.1 mm to 1 mm. In order to compare the flame changes around particles under different particle sizes, the length of the x-axis is taken as the ratio of particle distance and particle radius to make the length−diameter ratio consistent. Figure 6a shows that the high-temperature area of particles at particle size of 0.1 mm is concentrated in the middle of particles 1 and 2 and at the right end of particle 2 and that the peak temperature near the particles is 2071 K. As the particle dimensions increase, the peak temperature of char particles decreases gradually. When dimensions are 1 mm, the peak temperature of the particle decreases to 1768 K. When the particles are small, the heat transfer spreads more rapidly, so the temperature is higher than the large size particles. After the particle size increases, the high-temperature region around the particle gradually decreases, and the high-temperature region between the double particles gradually concentrates to the left end of particle 1 and pore of the particles.

The high temperature represents the strong reaction area. When the particle size is 0.1 mm, the relative flame layer is far from the particle surface. With the increase in particle size, the relative flame layer gradually is close to the particle surface, which also represents the change of reaction area. As the particle size increases by 0.1 mm to 1 mm, the reaction area gradually concentrates on the face and pores of coal char particles.

Figure 7a shows the total reaction rate of double coal char particles at various particle sizes. Figure 7a shows that the reaction rates from R1 to R7 all increase with the increase of coal size. As the size increases, the surface area of the particle

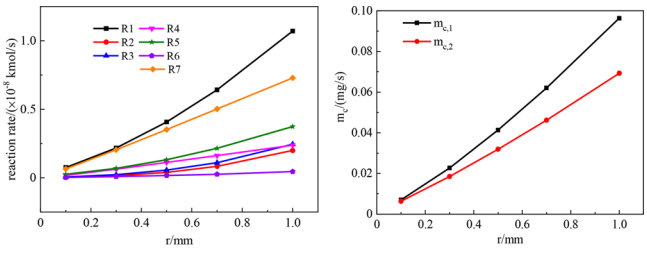

(a) Total reaction rate (b) Carbon consumption rate

Figure 7. Total reaction rate and carbon consumption rate of double coal char particles with different particle sizes.

increases greatly, the reaction site increases, and the reaction between the gas flow and the particle becomes active. R1 and R7 always dominate the reaction, and the reaction rate of R6 is the lowest. It shows that the combustion reaction of particles is dominant under these conditions.

Figure 7b represents the carbon consumption rate of double coal char particles with different particle sizes. Carbon consumption rate shows a linear increase as particle size increases. The carbon consumption rate of particle 1 is higher than particle 2. At the size of 0.1 mm, the carbon consumption rate of particle 1 is 0.00698 mg/s and that of particle 2 is 0.00632 mg/s; particle 1 is about 10.5% higher than particle 2. When the size is 1 mm, the carbon consumption rate of particle 1 is 0.09634 mg/s and that of particle 2 is 0.06924 mg/s, the carbon consumption rate of particle 1 is about 39% higher than that of particle 2. The increase of particle size makes the carbon consumption rate of double particles increase about 10 times. It is indicated that the particle size is an important element affecting the total carbon reaction rate. The reaction rate of the heterogeneous reaction mainly depends on the particle surface of the reaction activity; the particle size leads to an increase of heterogeneous reaction contact area, so the reaction activity sites and carbon consumption rate greatly increase. With the increase of particle size, the carbon consumption rate for particle 1 increases significantly faster than that for particle 2. Due to the larger particle size, more gas is consumed by particle 1, which reduces the concentration of reaction atmosphere attached to particle 2 and slows the growth of carbon consumption rate.

3.3. Different Distances under Various Sizes. The gas concentration ratio at the inlet is YH_2O:YO_2:YCO_2 = 0.05:0.2:0.75, and the temperature of the environment is T_∞ = 1500 K. The structure and particle size are the same for double coal char particles, and the particle distance L = 2.2r, 5r.

The effect of the variation of particle distance on the reaction characteristics for double coal char particles with the same particle size of r = 0.5 and 1 mm is investigated. Velocity field distribution, reaction rate, and carbon consumption rate for the particles with different particle distances are compared.

Figure 8 shows the velocity field distribution of double coal char particles with r = 0.5 mm and r = 1 mm at different particle distances. Figure 8a indicates the velocity field of coal char particle at particle distance L = 2.2r and particle size r = 0.5 mm. The gas-phase fluid flows from the left side of the particle to the right side, and the velocity around the particle is almost zero, while the velocity outward from the particle increases gradually. When the particle distance L is 2.2r, the velocity fields of the double particles are basically fused

https://doi.org/10.1021/acsomega.2c07675
ACS Omega 2023, 8, 7913−7921

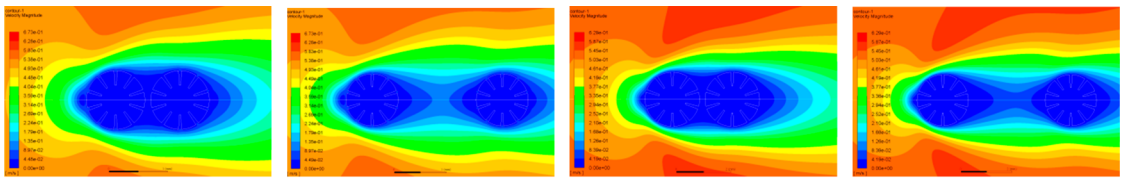

(a) r=0.5 mm, L=2.2 r (b) r=0.5 mm, L=5 r (c) r=1 mm, L=2.2 r (d) r=1 mm, L=5 r

Figure 8. Velocity field at different particle sizes and different distances.

together, and the fluid cannot pass through between the double particles. Figure 8b shows that when the particle distance L is 5r, the velocity field of the double particles is obviously separated, and part of the gas-phase fluid can pass through the middle of the double particles. Combining c and d in Figure 8, the distribution patterns for velocity fields with particle sizes of 0.5 and 1 mm are not significantly distinct at the same particle distance, but their values show a lot of change. The particle sizes increase from r = 0.5 mm to r = 1 mm, and maximum velocity values of the coal char velocity fields with different particle distance decrease from 0.673 to 0.629 m/s. Particle size is smaller, and the separation degree of velocity field is greater. The velocity field of small particles is more widely distributed, which is due to the small volume. At the same initial flow velocity, the flow is more easily diffused around the small particles, and the velocity value is also larger.

The gasification reaction of coal char particles consists of seven reactions, and the total reaction rate of the particles is obtained by integrating the reaction rate volumetrically for homogeneous reactions and area for heterogeneous reactions. Figure 9 shows the variation of the total reaction rate and

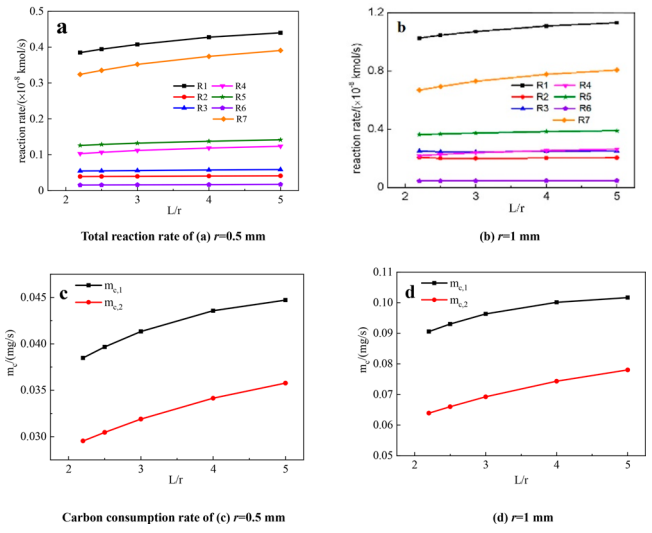

Figure 9. Total reaction rate and carbon consumption rate of double coal char particles with r = 0.5 mm and r = 1 mm at different particle distances.

carbon consumption rate for double coal char particles with particle size r = 0.5 mm and r = 1 mm with different particle distances. Figure 9a indicates that the reaction rates of reactions for coal char particles with r = 0.5 mm all increase with the increase of particle distance, while only R2 and R3 decrease first and then increase when r = 1 mm in Figure 9b. As the particle distances increase, the reaction rates of R1 and R7 grow much faster than those of the other five reactions. When particle size changes from R = 1 mm to r = 0.5 mm, the reaction rate of R1 is larger than R7, and R2 and R3 are improved to a greater extent. This indicates that the reaction characteristics of particles do not simply increase or decrease with different particle sizes even if the double particles are at the same distance.

Figure 9c,d presents the variation of carbon consumption rate for coal char particles with different particle distance. As seen from Figure 9c,d, the carbon consumption rate of double particles with different particle sizes showed an upward trend as the particle distance increased. For double particles whose size is 1 mm at particle distance of 2.2r, the carbon consumption rates for particle 1 and particle 2 are 0.0906 mg/s and 0.0639 mg/s, respectively. When the particle distance expanded to 5r, the carbon consumption rate for particle 1 and particle 2 reaches 0.1017 and 0.07085 mg/s, respectively. With increasing particle distance, the carbon consumption rate for char particles with particle size of 1 mm increased slightly less than that of 0.5 mm char particles.

4. CONCLUSIONS

This paper builds a reaction model of double coal char particles, and the model is compared with the literature for verification. The gasification reaction characteristics for double coal char particles under different particle distance and particle size are studied, and the conclusions are as follows:

(1) The data obtained by the porous particle model matches well with the experimental data, indicating that the model can almost represent the gasification reaction characteristics of coal char particles.

(2) The particle distance can affect the position for the high-temperature region and change the peak temperature for the high-temperature region. However, when the particle distance is large to a certain extent, the interaction between the particles is weakened and the characteristics of double char particles tend to be consistent with that of single particle. The temperature of particle 1 is more than that of particle 2. With the increase of particle distance, the reaction rate and carbon consumption rate for the double particles presented an upward trend.

(3) The increase in particle size leads to a decrease in the peak temperature of char particles. The particle size increases, the region of high temperature all over the particle decreases with the particle size, and the high-temperature region gradually transfers from the surroundings to the pore of the particle. The reaction rate and carbon consumption rate are faster as the particle size of coal increases. As the surface area of coal particles increases with the increase in particle size, the carbon consumption rate presents a linear upward trend. In addition, the carbon consumption rate for particle 1 is higher than that of particle 2.

https://doi.org/10.1021/acsomega.2c07675
ACS Omega 2023, 8, 7913−7921

(4) For small particles, the distance effect at the same degree is greater, because smaller size makes them more easily affected at the same airflow velocity. Small particles at the same distance have higher temperatures because they transfer heat faster. With the increase of particle distance, carbon consumption rates for double particles with different particle sizes show an increasing trend. The larger the particle size is, the slower the carbon consumption rate increases for the particle distance.

AUTHOR INFORMATION

Corresponding Author

Xudong Song − *State Key Laboratory of High-Efficiency Utilization of Coal and Green Chemical Engineering, School of Chemistry and Chemical Engineering, Ningxia University, Yinchuan, Ningxia 750021, China;* orcid.org/0000-0002-8211-409X; Email: xdsong@nxu.edu.cn

Authors

Weiguang Su − *State Key Laboratory of High-Efficiency Utilization of Coal and Green Chemical Engineering, School of Chemistry and Chemical Engineering, Ningxia University, Yinchuan, Ningxia 750021, China*

Meiyu Shi − *State Key Laboratory of High-Efficiency Utilization of Coal and Green Chemical Engineering, School of Chemistry and Chemical Engineering, Ningxia University, Yinchuan, Ningxia 750021, China*

Ben Zhang − *Xi'an Thermal Power Research Institute Co, Ltd, Xi'an, Shanxi 710032, China*

Wenxin Wang − *State Key Laboratory of High-Efficiency Utilization of Coal and Green Chemical Engineering, School of Chemistry and Chemical Engineering, Ningxia University, Yinchuan, Ningxia 750021, China*

Guangsuo Yu − *State Key Laboratory of High-Efficiency Utilization of Coal and Green Chemical Engineering, School of Chemistry and Chemical Engineering, Ningxia University, Yinchuan, Ningxia 750021, China; Institute of Clean Coal Technology, East China University of Science and Technology, Shanghai 200237, China;* orcid.org/0000-0003-4085-9736

Complete contact information is available at: https://pubs.acs.org/10.1021/acsomega.2c07675

Author Contributions

#W.S. and M.S. contributed equally to this work.

Notes

The authors declare no competing financial interest.

ACKNOWLEDGMENTS

The authors gratefully acknowledge the financial support received from the Key Researcher Plan of Ningxia (Grant Number 2019BCH01001) and the National Natural Science Foundation of China (Grant Numbers U21A20318 and 22108132).

REFERENCES

(1) Liu, J.; Chen, S.; Wang, H.; et al. Evolution of China's Urban Energy Consumption Structure-A Case Study in Beijing. *Energy Procedia.* **2016**, *88*, 88−93.

(2) Zhu, G.; Zhang, B.; Lv, B.; Yan, G.; Zhu, X. Clean desulphurization of high-sulfur coal based on synergy effect between microwave pretreatment and magnetic separation. *ACS Omega.* **2018**, *3*, 10374−10382.

(3) Zhang, L.; Gao, W.; Chiu, Y.; et al. Environmental performance indicators of china's coal mining industry: a bootstrapping malmquist index analysis. *Resour. Policy.* **2021**, *71*, 101991−101999.

(4) Liu, S.; He, F.; Zhao, K.; Zhao, H.; Huang, Z.; Wei, G.; Yang, W. Long-term coal chemical looping gasification using a bimetallic oxygen carrier of natural hematite and copper ore. *Fuel.* **2022**, *309*, 122106−122116.

(5) Otoshi, A.; Sasaki, K.; Anggara, F. Screening of UCG chemical reactions and numerical simulation up-scaling of coal seam from laboratory models. *Combust. Theory model.* **2022**, *26*, 25.

(6) Zeng, L.; He, F.; Li, F.; et al. Coal-Direct Chemical Looping Gasification for Hydrogen Production: Reactor Modeling and Process Simulation. *Energy Fuel.* **2012**, *26*, 3680−3690.

(7) Asif, M.; Bak, C.-u; Saleem, M. W.; Kim, W.-S. Performance Evaluation of Integrated Gasification Combined Cycle (IGCC) Utilizing a Blended Solution of Ammonia and 2-amino-2-methyl-1-propanol (AMP) for CO_2 Capture. *Fuel.* **2015**, *160*, 513−524.

(8) Bing, X.; Wang, Z.; Wei, F.; Gao, J.; Wang, Y.; et al. Separation of m -Cresol from Coal Tar Model Oil Using Propylamine-Based Ionic Liquids: Extraction and Interaction Mechanism Exploration. *ACS Omega.* **2020**, *5*, 23090−23098.

(9) Wang, B.; Qiu, J.; Guo, Q.; Gong, Y.; Xu, J.; Yu, G. Numerical Simulations of Solidification Characteristics of Molten Slag Droplets in Radiant Syngas Coolers for Entrained-Flow Coal Gasification. *ACS Omega.* **2021**, *6*, 20388−20397.

(10) Senneca, O.; Urciuolo, M.; Bareschino, P.; et al. Pyrolysis, combustion, and fragmentation model of coal particles: preliminary results. *Combust. Sci. Technol.* **2016**, *188*, 759−768.

(11) Niksa, S.; Mitchell, R.; Hencken, K.; et al. Optically determined temperatures, sizes, and velocities of individual carbon particles under typical combustion conditions. *Combust. Flame* **1985**, *60*, 183−193.

(12) Zhu, M.; Zhang, H.; Tang, G.; et al. Ignition of single coal particle in a hot furnace under normal- and micro-gravity condition. *Proc. Combust. Inst.* **2009**, *32*, 2029−2035.

(13) Si, M.; Cheng, Q.; Yuan, L.; et al. High Temporal−spatial distribution of soot temperature and volume fraction in single coal combustion flame. *Combust. Sci. Technol.* **2022**, *194*, 3246.

(14) Wang, Y.; Zou, C.; Zhao, J.; Wang, F. Combustion Characteristics of Coal for Pulverized Coal Injection (PCI) Blending with Steel Plant Flying Dust and Waste Oil Sludge. *ACS Omega.* **2021**, *6*, 28548−28560.

(15) Levendis, Y.; Joshi, K.; Khatami, R.; et al. Combustion Behavior in air of single particles from three different coal ranks and from sugarcane bagasse. *Combust. Flame* **2011**, *158*, 452−465.

(16) Khatami, R.; Stivers, C.; Joshi, K.; et al. Combustion behavior of single particles from three different coal ranks and from sugar cane bagasse in O_2/N_2 and O_2/CO_2 atmospheres. *Combust. Flame* **2012**, *159*, 1253−1271.

(17) Khatami, R.; Levendis, Y. An overview of coal rank influence on ignition and combustion phenomena at the particle level. *Combust. Flame* **2016**, *164*, 22−34.

(18) Higuera, F. Combustion of a coal char particle in a stream of dry gas. *Combust. Flame* **2008**, *152*, 230−244.

(19) Nikrityuk, P.; Kestel, M.; Meyer, B.; et al. Numerical study of the influence of heterogeneous kinetics on the carbon consumption by oxidation of a single coal particle. *Fuel.* **2013**, *114*, 88−98.

(20) Richter, A.; Nikrityuk, P.; Kestel, M. Numerical investigation of a chemically reacting carbon particle moving in a hot O_2/CO_2 atmosphere. *Ind. Eng. Chem. Res.* **2013**, *52*, 5815−5824.

(21) Richter, A.; Nikrityuk, P.; Meyer, B. Three-dimensional calculation of a chemically reacting porous particle moving in a hot O_2/CO_2 atmosphere. *Int. J. Heat Mass Transfer* **2015**, *83*, 244−258.

(22) Dierich, F.; Richter, A.; Nikrityuk, P. A fixed-grid model to track the interface and porosity of a chemically reacting moving char particle. *Chem. Eng. Sci.* **2018**, *175*, 296−305.

(23) Bejarano, P.; Levendis, Y. Combustion of coal chars in oxygen-enriched atmospheres. *Combust. Sci. Technol.* **2007**, *179*, 1569−1587.

(24) Richter, A.; Vascellari, M.; Nikrityuk, P.; et al. Detailed analysis of reacting particles in an entrained-flow gasifier. *Fuel Process. Technol.* **2016**, *144*, 95−108.
(25) Coetzee, G.; Sakurovs, R.; Neomagus, H.; et al. Particle size influence on the pore development of nanopores in coal gasification chars: From micron to millimeter particles. *Carbon.* **2017**, *112*, 37−46.
(26) Xue, Z.; Guo, Q.; Gong, Y.; et al. Numerical study of a reacting single coal char particle with different pore structures moving in a hot O_2/CO_2 atmosphere. *Fuel.* **2017**, *206*, 381−389.
(27) Standnes, D. Dissipation Mechanisms for Fluids and Objects in Relative Motion Described by the Navier−Stokes Equation. *ACS Omega.* **2021**, *6*, 18598.
(28) Niu, Y.; Wang, S.; Shaddix, C.; et al. Kinetic modeling of the formation and growth of inorganic nano-particles during pulverized coal char combustion in O_2/N_2 and O_2 $/CO_2$ atmospheres. *Combust. Flame* **2016**, *173*, 195−207.
(29) Turns, S. *An introduction to combustion: Concepts and applications*, 2nd ed.; McGraw-Hill: Boston, MA, 2000.
(30) Jones, W.; Lindstedt, R. Global reaction schemes for hydrocarbon combustion. *Combust. Flame* **1988**, *73*, 233−249.
(31) Caram, H.; Amundson, N. Diffusion and reaction in a stagnant boundary layer about a carbon particle. *Ind. Eng. Chem. Fundam.* **1977**, *16*, 171−181.
(32) Libby, P.; Blake, T. Burning carbon particles in the presence of water vapor. *Combust. Flame* **1981**, *41*, 123−147.
(33) Date, A. *Introduction to computational fluid dynamics*; Cambridge University Press: New York, 2005.
(34) Zhou, Y.; Jin, X.; Chu, W. Quantitative measurement and indication of pulverized coal ignition temperatures in O_2/CO_2 environments. *Appl. Therm. Eng.* **2017**, *112*, 888−894.

https://doi.org/10.1021/acsomega.2c07675
ACS Omega 2023, 8, 7913−7921